Atmos. Chem. Phys. Discuss., 9, 21819–21846, 2009
www.atmos-chem-phys-discuss.net/9/21819/2009/

Atmospheric Chemistry and Physics Discussions

This discussion paper is/has been under review for the journal *Atmospheric Chemistry and Physics (ACP)*. Please refer to the corresponding final paper in *ACP* if available.

On the seasonal dependence of tropical lower-stratospheric temperature trends

Q. Fu[1], **S. Solomon**[2], **and P. Lin**[1]

[1]Department of Atmospheric Sciences, University of Washington, Seattle, WA, USA
[2]Chemical Science Division, Earth System Research Laboratory, NOAA, Boulder, CO, USA

Received: 14 August 2009 – Accepted: 30 September 2009 – Published: 16 October 2009

Correspondence to: Q. Fu (qfu@atmos.washington.edu)

Published by Copernicus Publications on behalf of the European Geosciences Union.

Abstract

This study examines the seasonality of tropical lower-stratospheric temperature trends using the Microwave Sounding Unit lower-stratospheric channel (T_4) for 1979–2007. We present evidence that this seasonality is a response to changes in the Brewer–Dobson circulation (BDC) driven by extratropical wave forcing. We show how the tropical T_4 trend can be used as an indicator of the change in the BDC, and find that the BDC is strengthening for 1979–2007 in June–November related to the Southern Hemisphere (SH) and in December–February to the Northern Hemisphere (NH). In marked contrast, we find that the BDC is weakening in March–May, apparently because of a weakening of its northern cell. The novel observational evidence on the seasonal dependence of the BDC trends presented in this study has important implications for the understanding of climate change in the stratosphere as well as testing climate model simulations.

1 Introduction

The Brewer–Dobson circulation (BDC) is the Lagrangian-mean mass circulation in the stratosphere, which consists of a meridional cell in each hemisphere with air rising across the tropical tropopause, moving poleward, and sinking to the extratropical troposphere. The BDC is driven remotely by planetary and gravity wave breaking in the extratropical stratosphere, which acts like a "suction pump" drawing air upward from the tropics (Haynes et al., 1991; Holton et al., 1995). In an analysis of the lower-stratospheric temperatures of the microwave sounding unit (MSU) channel 4 (T_4), Yulaeva et al. (1994) showed a nearly complete compensation between temperature changes in the tropics and in the extratropics on the month-to-month time scale and for the annual cycle. They interpreted these out-of-phase temperature variations between the tropics and extratropics as the signature of the variations of the BDC driven by extra-tropical wave forcing. Here we show that similar considerations are key to un-

ACPD

9, 21819–21846, 2009

derstanding decadal changes in stratospheric temperature and circulation, particularly their seasonal character.

GCMs with detailed representations of the stratosphere (e.g., Sigmond et al., 2008) predict a stronger BDC in response to an increase in wave activity associated with a rising greenhouse gas concentrations as well as ozone depletion (e.g. Ramaswamy et al., 1996; Rind et al., 2001; Eichelberger and Hartmann, 2005; Butchart et al., 2006; Li et al., 2008). By comparing a number of middle atmosphere GCM simulations, Butchart et al. (2006) suggested that despite considerable inter-model variability a positive trend in the tropical upward mass flux was a robust feature in the models examined, and it occurred throughout the year. On the other hand, a coupled chemistry-climate model study of Li et al. (2008) found that in the past few decades, nearly half of the tropical upward mass flux increase occurred in December–February and that both hemispheres contributed equally to these changes.

Since temperature variations in the lower stratosphere are strongly related to the residual vertical velocities (Yulaeva et al., 1994; Randel et al., 2006), the consequence of an accelerated BDC is an additional cooling of the lower tropical stratosphere but warming in the high latitudes. Observational evidence of an accelerated BDC has been shown over both the tropics (e.g., Rosenlof and Rind, 2008) and high latitudes (Johanson and Fu, 2007; Lin et al., 2009) in terms of changes in lower-stratospheric temperatures. However, there is no observational study so far that examined the seasonal dependence of the long-term changes in the BDC and their partitioning between its northern and southern cells. Such study can provide key tests of GCM predictions and improve our understanding of the climate change-induced evolution of the BDC.

The purpose of this paper is to address BDC changes using the observed seasonality of the lower-stratospheric temperature trends. Note that a strengthening of the BDC means a faster tropical upwelling, which leads to a cooling in the tropical lower stratosphere. In this study, we will show evidence that the seasonal dependence of observed lower-stratospheric temperature trends in the tropics is almost entirely driven by the changes in the BDC. We will also estimate the direct radiative contribution to

the cooling in the tropical lower-stratosphere. Our analysis suggests that the BDC is strengthening since 1979 in June–February but weakening in March–May.

This paper is organized as follows. Section 2 describes the data used in this study. The general trend features in the lower-stratospheric temperature are presented in Sect. 3. The analysis method and results are shown in Sect. 4. The discussion and conclusions are given in Sect. 5.

2 Data

For the analysis of the lower-stratospheric temperature trends, we used the MSU/AMSU lower-stratospheric channel monthly brightness temperature (T_4) gridded (2.5°×2.5°) data (version 3.0) compiled by the Remote Sensing System (RSS) for 1979–2007 (Mears et al., 2003). The T_4 weighting function ranges from ~20 hPa to ~120 hPa and peaks at around 60–70 hPa (e.g., Fu and Johanson, 2005), which thus well represents the lower stratosphere. The MSU measurements extend to 82.5° N(S). Although we mainly use the RSS T_4 data in this study, consistent results are obtained using the T_4 data from the University of Alabama at Huntsville (UAH) team (Christy et al., 2003). The comparisons between results from these two datasets will be shown in Fig. 1 and discussed further in Sect. 4. Note that only RSS data will be used in results presented in Figs. 2–11.

To examine the ozone trend patterns, we used the monthly mean total column ozone gridded (1°×1.25°) data (version 8) from the Total Ozone Mapping Spectrometer (TOMS) for 1979–2007. The merged TOMS/SBUV (Solar Backscatter Ultraviolet) dataset (Stolarski et al., 2006) is regarded as a more reliable record that has the benefit of external calibration. It also partly fills the data gap between 1993–1995 but it has lower resolution (5°×10°). In our study we found that the spatial patterns of the trends observed since 1979 do not differ significantly between the two datasets. Therefore, we used the TOMS to produce trend maps but the TOMS/SBUV to generate area-weighted spatially averaged ozone time series.

ACPD
9, 21819–21846, 2009

The National Center for Environmental Prediction/National Center for Atmospheric Research (NCEP/NCAR) reanalysis data (Kalnay et al., 1996) was used to calculate the eddy heat flux as an index for the strength of the BDC. The close agreement between the NCEP/NCAR reanalysis and the MSU observations in the SH high latitudes in terms of stratospheric temperature trend patterns (Hu and Fu, 2009; Lin et al., 2009) lends confidence to the analysis of trends in SH wave activity.

We examined the GCM simulations by using those performed in support of the IPCC AR4 (Meehl et al. 2007) from the World Climate Research Programme's (WCRP's) Coupled Model Intercomparison Project phase 3 (CMIP3) multi-model dataset archive. There are 22 GCM simulations containing 48 ensembles, which all considered the long-lived greenhouse gas increases. Among them there are 13 models composing 28 ensembles that also considered stratospheric ozone depletion. Two sets of simulations are combined to get a full record from 1979 to 2007: one is from the 20th century experiment (20C3M), and the other is from the SRES A1B simulations that are initialized from the corresponding 20C3M ensembles at the end of 20th century. Simulated T_4 is derived by averaging the vertical profile of temperature using the MSU T_4 weighting function. In this study we considered the ensemble mean of GCM simulations that incorporated ozone depletion.

3 General trend features

In this study we define the tropics from 20° S to 20° N and high latitudes from 40° N(S)–82.5° N(S). Figure 1 shows the monthly dependence of the observed T_4 trend (solid lines) in the tropics for 1979–2007. Using the RSS (UAH) dataset, it has a minimum cooling of −0.04 K/decade (−0.1 K/decade) in March but a large cooling of about −0.42 K/decade (−0.5 K/decade) from July to January, with an annual mean trend of −0.31 K/decade (−0.38 K/decade). The dashed lines indicate our estimates of the T_4 cooling due to direct radiative forcing as will be derived later based on observations, which bracket the dotted line showing the total T_4 trend simulated by the suite of IPCC

AR4 models.

Figure 2a shows the zonal mean T_4 trends for 1979–2007 versus month and latitude. A slight warming is seen between 10° N–20° N in March. Since this warming must be a result of the combination of the direct radiative cooling induced by ozone depletion and greenhouse gas increases and the temperature changes due to vertical motion changes, it is indicative of a significant dynamic warming in March in the tropics due to decreased upward motion. This is consistent with a strong cooling in the NH high-latitudes in the same month, which should also be largely dynamically driven. Figure 2a also shows T_4 warmings in the SH high-latitude winter/spring seasons and in the NH high-latitude winter. Since these warmings cannot be explained by the direct radiative forcing that induces cooling in last three decades (e.g., Shine et al., 2003; Ramaswamy et al., 2006), they provide a unique fingerprint of the strengthening of the BDC.

In Fig. 2a the insignificant (or near zero) T_4 trend in the tropics in the NH spring is due to the cancellation of the radiative cooling and dynamic warming. The same argument is applied to the insignificant zonal mean trend in the SH high latitudes in the SH winter and spring. The large warming with little shading region in the NH high latitudes in the NH winter is due to the large natural variability as well as the cancellation of the radiative cooling and dynamic warming there.

Figure 2b is the same as Fig. 2a except from the IPCC AR4 GCM simulations that consider ozone depletion. It suggests that these GCM simulations do not catch the T_4 trends associated with the change of the BDC. More discussion of the model simulations versus observations will be given in Sect. 5.

4 Analyses and results

In this section, we will present evidence that the seasonality of the tropical T_4 trend (solid line in Fig. 1) is almost entirely caused by the seasonality in the changes in the BDC. We will then derive the contribution of direct radiative cooling to the trend in tropical T_4 based on observations. For these purposes, we will first quantify the high

latitude T_4 trends due to the change of the BDC and then relate them to changes linked to tropical upwelling, presumably through the downward control principle (Haynes et al., 1991; Yulaeva et al., 1994; Holton et al., 1995).

4.1 T_4 trends over SH high latitudes due to dynamics only

The T_4 trend patterns in the SH high latitudes in the winter and spring (June–November) exhibit a great deal of zonal asymmetry, with substantial net warming over significant parts of SH high latitudes (see Fig. 3). The small zonal mean trend (Fig. 2a), especially in September and October, represents a small residual due to the incomplete cancellation of much larger regional warming and cooling trends that are both statistically significant (Hu and Fu, 2009; Lin et al., 2009). Consistent trend patterns in the SH winter and spring are also found regardless of the ending years uses (e.g., 1979–1995, . . . , 1979–2001, . . . , 1979–2007), indicating that the observed trend patterns in Fig. 3 are not unduly influenced by the effect of unusual years such as 2002. The observed trend patterns can be attributed to a combination of ozone-depletion-induced radiative cooling, BDC-acceleration-induced dynamic warming, and accompanying changes in the polar stationary planetary wavenumber-1 (Lin et al., 2009). The latter has little impact on the zonal-mean trend.

Following Lin et al. (2009), we use the multiple regression method to separate the BDC-induced T_4 trend from the ozone-induced radiative trend in June–October (see Fig. 3). An "ozone index" is defined as the area-weighted spatial-mean total ozone over 40° S poleward to represent the ozone-induced radiative effect. The eddy heat flux (equivalent to the vertical component of the Eliassen–Palm flux) in the lower stratosphere is often used as a measure of the BDC (Andrews et al., 1987). Herein an "eddy heat flux index" is defined to represent the BDC strength, which is the two-month mean area-weighted averaged eddy heat flux at the 150 hPa over 40° S–90° S. The two-month mean is two thirds from previous month and one third from current month following Ueyama and Wallace (2009).

The eddy heat flux in the previous month is included since it may contribute to the

dynamical heating in the current month (e.g., Hu and Tung, 2002). The eddy heat flux at 150 hPa represents how much wave activity has propagated from troposphere to stratosphere. Since most of these waves will break in the upper stratosphere, the eddy heat flux below should be quite similar (e.g., the correlation of eddy heat flux among different levels between 150 and 50 hPa are never lower than 0.9). The eddy heat flux at 150 hPa is thus proportional to wave divergence in the upper stratosphere. Most eddy heat flux in the lower stratosphere is within 40–70° latitude. Thus including the polar region or not has little effect on the calculated spatial-averaged eddy heat flux. The advantage of including the polar region is that the total flux over 40–90° latitudes is equivalent to the convergence of the eddy heat flux over the whole area because there is no flux at the pole (e.g., Hu and Tung, 2002).

In addition to the eddy heat flux, Ueyama and Wallace (2009) used a zonal wind index to measure the strength of the BDC. It is defined as the area-weighted spatial-mean zonal wind over the lower part of the stratospheric jet region (40–70° S, 20–10 hPa). We find that the results using the "eddy heat flux index" and "zonal wind index" agree well. Herein we only show results using the "eddy heat flux index".

Multiple regression of gridded monthly-mean T_4 data is performed upon the two standardized time series of the indices. The regression maps represent patterns of temperature anomalies that are linearly correlated with one standard deviation anomaly in the indices. The attribution of the T_4 trend to changes in ozone concentration and the BDC strength is thus obtained by multiplying the regression maps by the linear trend in the corresponding standardized index.

As an example, Fig. 4 shows the time series of the eddy heat flux (a) and ozone (b) indices in September and their corresponding regression maps (c and d) in units of K per unit standard deviation of these indices. Figure 5 shows the observed September T_4 trend (a) and the contributions to the T_4 trend due to the changes in the BDC (b) and ozone (c). The summation of (b) and (c) is shown in (d), which captures the observed trend pattern well. The residual (i.e., the observed trend minus the combined trend) shown in (e) is small over most of the SH high latitudes: The spatial mean of the

residual over SH high latitudes is actually zero. It indicates that the temperature change on the decadal timescale is indeed largely driven by changes in ozone concentration and BDC in September.

We carried out a similar multiple regression for the November data. But the derived BDC-induced trend is near zero in this month, which is obviously incorrect as evidenced by the warming in November (Fig. 3). This may be because the sub-grid gravity wave contribution to the eddy heat flux, which cannot be considered using the resolved fields from the reanalysis, may be important in this month. Further research is required to examine this issue.

Thus we applied a regression of gridded monthly-mean T_4 data upon the ozone index in November, which we call the single regression. The contribution to the T_4 trend due to changes in ozone is thus obtained by multiplying the regression maps by the linear trend of the ozone index. The BDC-induced trend is then derived by subtracting the ozone contribution from the total trend.

The results using single and multiple regression methods are compared by applying both methods to 12 months of the year. It is found that they agree with each other well in all months except November. Furthermore Fig. 3 suggests that the dynamic warmings in December-May are near zero, which is also indicated in both analyses although those from the single-regression are generally closer to zero. Thus in this study, we choose to combine the single and multiple regression methods, which are, respectively, applied to November–May and June–October. Note that December-May are months when the ozone-depletion-induced cooling plays a dominant role (Fig. 3).

The T_4 trend due to the changing BDC, averaged over SH high latitudes (40° S–82.5° S), is shown in Fig. 6 (dashed line) versus the month of the year. The trend has a maximum warming of 0.75 K/decade in September, and is positive from June through November. It is near zero in December–May.

ACPD
9, 21819–21846, 2009

4.2 T_4 trends over NH high latitudes due to dynamics only

The zonal mean trend in NH high latitudes (Fig. 2a) shows very strong warming during the winter, which must be driven by dynamics, i.e., adiabatic compression associated with a stronger BDC. However, the NH also displays strong zonal mean cooling in the spring (March–April), which is as strong as that in the SH spring. This is very unlikely to be due to ozone loss since the ozone losses in the Arctic are much smaller than in the Antarctic (see Fig. 7 vs. Fig. 3). Further, tropical net warming is observed in March, proving important evidence that the cooling in NH spring is due to a reduction in the strength of the BDC (Fig. 2). In the summer, since the effect of the BDC on the NH high latitudes is small (e.g., Yulaeva et al., 1994), the cooling (Fig. 2) in this season must be largely caused by direct radiative forcing.

The eddy heat flux derived from reanalysis fields may not be reliable in NH since the subgrid gravity waves play a critical role in driving BDC there. Furthermore we have less confidence on the NCEP/NCAR reanalysis in the NH than in the SH. Note that the annual mean T_4 trends from NCEP/NCAR reanalysis are 85 and 20% different from MSU observations in the NH and SH high latitudes, respectively.

Since there is no ozone hole in the NH high latitudes, we expect much less seasonal dependence of radiatively induced T_4 trends there. Note that the seasonal dependence of the O_3 trends (e.g., more negative in March–April but less in December–January as shown in Fig. 7) is largely caused by the change of the BDC. But the radiative effect of the ozone change caused by the BDC change is at least one order of magnitude smaller than its direct dynamic effect on T_4 (Yulaeva et al., 1994). Thus in this study we simply assume a constant radiatively induced T_4 trend in NH high latitudes, which is the mean T_4 trend in June–August (-0.32 K/decade). For comparison, the radiatively induced cooling over SH high latitudes is about -0.34 K/decade in February–July when the ozone hole has little effect. Since radiatively induced T_4 trend in NH high latitudes should not be larger than that in the SH high latitudes, the dynamic warming in the NH summer if any should not be significantly larger than about 0.02 K/decade.

ACPD
9, 21819–21846, 2009

Thus we estimate the NH high latitude trends due to dynamics by subtracting the mean cooling in June–August from the total trend in each month. Figure 6 indicates that the dynamic warming in NH high latitudes (dotted line) is small from May to November. It becomes large in December (0.55 K/decade) and January (0.65 K/decade). As already noted, there is a large cooling in March (−0.47 K/decade), which appears to be coupled with the dynamic warming in the tropics in the same month.

4.3 Coupling of tropical T_4 trend and high-latitude dynamical T_4 trend

The estimated high-latitude T_4 trend due to dynamics only is shown in Fig. 6 (the solid line) which is the average of the dynamically-induced SH and NH high-latitude trends. This trend is normalized and shown in Fig. 8 versus month as compared with the normalized tropical T_4 trends multiplied by (−1). The normalized trend is defined as $(x_i - \bar{x}) / \left(\sum_{i=1}^{12} (x_i - \bar{x})^2 / 12 \right)^{1/2}$ where x_i is the trend for a given month and $\bar{x}$ is the annual mean trend. Figure 8 indicates a nearly complete compensation between these two normalized trends. The close coupling between the tropical T_4 trend and the high-latitude dynamically induced T_4 trend can be understood as a response of the lower-stratospheric temperature to the change in the BDC driven by extratropical wave forcing. Figure 8 suggests that the seasonal dependence of the T_4 trend in the tropics is almost entirely driven by dynamics.

We can relate the T_4 trend in the tropics (solid line in Fig. 1) to the dynamically induced T_4 trend in high latitudes (solid line in Fig. 6) by least-square fitting

$$T_{4,\text{Tropics}} = -0.20 - 0.78 \times T_{4,\text{High-Lat,dynamics only}} \quad (1)$$

Note that the correlation coefficient r is −0.97 (see Fig. 9). Equation (1) suggests a T_4 trend of −0.20 K/decade in the tropics when the impact of the dynamics is zero, which can thus be interpreted as a radiatively-driven cooling (the dashed line in Fig. 1).

We tested the sensitivity of Eq. (1) to various methods used to derive the dynamic induced T_4 trends in high latitudes. By applying the multiple regression method to all

12 months of the year over SH high latitudes, we obtain a cooling of −0.20 K/decade with r=−0.91. The smaller correlation coefficient is due to the underestimation of the dynamic warming in November. Very similar results are obtained by applying a single regression on the ozone index to all months of the year (−0.21 K/decade with r=−0.95).

For the NH high latitudes, the radiatively induced cooling may be smaller in the late fall and winter than that in summer. In a sensitivity test, we reduce the radiatively induced cooling in October–January by 30% instead of using a constant radiative cooling throughout the year, which leads to a tropical radiative cooling of −0.21 K/decade with r=−0.96. In another sensitivity test by assuming a dynamic warming of 0.02 K/decade in NH summer, we obtain a tropical radiative cooling of −0.19 K/decade with r=−0.97.

Therefore we conclude that the radiative T_4 trend in tropics as derived from Eq. (1) is about −0.20±0.01 K/decade, which is robust and insensitive to various methods used to derive the dynamically induced T_4 trends in high latitudes. Using the trend of −0.20 K/decade as a reference level, Fig. 1 shows that the BDC is becoming stronger in NH summer, fall, and winter but weakening in NH spring.

It is worth mentioning that the correlation between the tropical monthly T_4 trends and those in high latitudes without removing the direct radiative effects is −0.75. Such correlation is already large enough to indicate the strong coupling in the decadal change of lower stratospheric temperatures between the tropics and high latitudes. By simply removing the direct radiative effect due to the ozone depletions in the SH high latitudes, which has strong seasonal dependence, the correlation becomes −0.97.

Although the RSS MSU data are used in this study, consistent results are obtained by using the MSU T_4 data from the University of Alabama at Huntsville (UAH) team (Christy et al., 2003). Note that the UAH T_4 trends are more negative than the RSS T_4 trends. Using the UAH data, the T_4 trend in the tropics due to the direct radiative effects is −0.29 K/decade (r=−0.97), which also indicates that the BDC is strengthening in NH summer, fall, and winter but weakening in NH spring (see Fig. 1).

It should be noted that the changes in BDC may lead to changes in the ozone field

ACPD
9, 21819–21846, 2009

which again may change the radiation and then the lower-stratospheric temperature. Such effect may be significant in the tropics (Yulaeva et al. 2009). This response is effectively considered as part of the BDC-induced trends in this study.

5 Discussion and conclusions

GCMs with detailed representations of the stratosphere suggest that the BDC is intensifying throughout the year (e.g., Butchart et al., 2006; Li et al., 2008). Using Eq. (1), we derived the tropical MSU T_4 trend due to the change of the BDC as well as the contribution from each hemisphere. The mean results for four seasons are shown in Fig. 10. The observations reveal the dynamically-induced cooling related to the strengthening of the BDC in JJA, SON, and DJF, in agreement with the model results. But the observations also show a dynamic warming in MAM, indicating a weakening of the BDC in that season, which contrasts with published models. Furthermore, Fig. 10 suggests that the change of the BDC in the last three decades in JJA and SON is dominated by the SH, while the change in DJF and MAM is related to the NH.

The coupled atmosphere-ocean climate models used in the IPCC AR4 generally do not have well-represented stratospheres so that the change of the BDC is unlikely to be captured. Instead the simulated T_4 trends in the past 30 years from these models closely follow the radiatively induced T_4 trends as derived from observations (Fig. 11). Such overall agreement lends confidence in derived radiatively induced T_4 trends from both GCMs and our observational analyses. Note that the IPCC AR4 models may underestimate the ozone-depletion induced radiative cooling in SH spring but overestimate it in SH summer and early fall. Also note that the observed Arctic cooling in March far exceeds that expected from the IPCC models despite their consideration of ozone losses (Figs. 2 and 11).

Rosenlof and Reid (2008) recently analyzed the long-term trends in tropical lower-stratospheric temperatures observed by radiosondes. They found a significant anticorrelation over the tropical western Pacific Ocean between the lower-stratospheric tem-

ACPD
9, 21819–21846, 2009

peratures and SST anomalies. It was suggested that tropical convection may be the link between the ocean and the stratosphere, and the increased stratospheric cooling may be an indication of strengthening tropical convection due to the SST increase. The idea of local forcing is consistent with the analysis by Kerr-Munslow and Norton (2006) who showed that tropical lower-stratospheric upwelling can be modulated by the upward flux of equatorial planetary wave activity. Deckert and Dameris (2008) suggested that this flux may be increasing as tropical SSTs rise and the latent heat release increases. The close coupling between the tropics and high latitudes in the decadal variations of the lower-stratospheric temperatures shown in this study, however, seemly indicates that enhanced tropical lower-stratospheric cooling is dominated by the strengthening of the BDC driven by an increase in extratropical wave forcing instead of a local one. One plausible interpretation of the observational results by Rosenlof and Reid (2008) is a mechanism linking changes in tropical SST to modulation of extra-tropical wave activity through changes in the meridional temperature gradient.

This study examines the seasonality of the tropical lower-stratospheric temperature trend, which is found to be almost entirely driven by changes in the BDC. We also estimate the lower stratospheric cooling in the tropics due to the direct radiative effects which is −0.20 K/decade (−0.29 K/decade) using the RSS (UAH) MSU data. Using the tropical lower-stratospheric temperature trends as an indicator of the change in the BDC, we find that the strengthening of the BDC since 1979 occurs in June–November related to the SH cell and in December–February related to the NH cell. We also find the BDC is weakening in March–May because of a weakening of the northern cell.

The present study provides observational evidence that decadal variations in the tropical lower-stratospheric temperatures and those in high latitudes are strongly coupled through the change of the BDC. Other studies suggest such couplings on the seasonal and inter-annual time scales (e.g., Yulaeva et al., 1994; Salby and Callaghan, 2002; Chae and Sherwood, 2007; Ueyama and Wallace, 2009). These results, however, may be in violation of the downward control principle that predicts that on time scales longer than the radiative relaxation time, the response to wave breaking should

be local in the latitude domain (Holton et al., 1995). Further research is required to reconcile these observational results with the conventional interpretation of the downward control principle.

Finally a recent observational study that examined the stratospheric air age (Engel et al., 2009) indicates a slight weakening of the annual mean BDC in last three decades. This contrasts with our results that suggests a strengthening of the annual mean BDC. Further research is also required to reconcile the differences between these two observational analyses.

Acknowledgements. We thank J. M. Wallace, K. H. Rosenlof and R. Ueyama for useful discussions. This work is supported by NOAA Grant NA08OAR4310725 and NASA Grants NNX08AG91G and NNX08AF66G.

References

Andrews, D. G., Holton, J. R., and Leovy, C. B.: Middle Atmosphere Dynamics, Academic Press, Orlando, United States, 489 pp., 1987.

Butchart, N., Scaife, A. A., Bourqui, M., de Grandpre, J., Hare, S. H. E., Kettleborough, J., Langematz, U., Manzini, E., Sassi, F., Shibata, K., Shindell, D., and Sigmond M.: Simulations of anthropogenic change in the strength of the Brewer–Dobson circulation, Clim. Dynam., 27, 727–741, doi:10.1007/s00382-006-0162-4, 2006.

Chae, H. C. and Sherwood, S. C.: Annual temperature cycle of the tropical tropopause: A simple model study, J. Geophys. Res., 112, D19111, doi:10.1029/2006JD007956, 2007.

Christy, J. R., Spencer, R. W., Norris, W. B., Braswell, W. D., and Parker, D. E.: Error estimates of version 5.0 of MSU-AMSU bulk atmospheric temperatures, J. Atmos. Ocean. Tech., 20, 613–629, 2003.

Deckert, R. and Dameris, M.: Higher tropical SSTs strengthen the tropical upwelling via deep convection, Geophys. Res. Lett., 35, L10813, doi:10.1029/2008GL033719, 2008.

Eichelberger, S. J. and Hartmann, D. L.: Changes in the strength of the Brewer–Dobson Circulation in a simple AGCM, Geophys. Res. Lett., 32, L15807, doi: 10.1029/2005GL022924, 2005.

Engel, A., Mobius, T., Bonisch, H., et al.: Age of stratospheric air unchanged within uncertainties over the past 30 years, Nature Geosci., 2, 28–31, 2009.
Fu, Q. and Johanson, C. M.: Satellite-derived vertical dependence of tropical tropospheric temperature trends, Geophys. Res. Lett., 32, L10703, doi:10.1029/2004GL022266, 2005.
Haynes, P. H., Marks, C. J., McIntyre, M. E., Shepherd, T. G., and Shine, K. P.: On the "downward control" of extratropical diabatic circulations by eddy-induced mean zonal forces, J. Atmos. Sci., 48, 651–678, 1991.
Holton, J. R., Haynes, P. H., McIntyre, M. E., Douglass, A. R., Rood, R. B., and Pfister, L.: Stratosphere-troposphere exchange, Rev. Geophys., 33, 403–439, 1995.
Hu, Y. and Tung, K. K.: Interannual and decadal variations of planetary wave activity, stratospheric cooling, and Northern Hemisphere annual mode, J. Climate, 15, 1659–1673, 2002.
Hu, Y. and Fu, Q.: Stratospheric warming in Southern Hemisphere high latitudes since 1979, Atmos. Chem. Phys., 9, 4329–4340, 2009, http://www.atmos-chem-phys.net/9/4329/2009/.
Johanson, C. M. and Fu, Q.: Antarctic atmospheric temperature trend patterns from satellite observations, Geophys. Res. Lett., 34, L12703, doi:10.1029/2006GL029108, 2007.
Kalnay, E., Kanamitsu, M., Kistler, R., Collins, W., Deaven, D., Gandin, L., Iredell, M., Saha, S., White, C., Woollen, J., Zhu, Y., Chelliah, M., Ebisuzaki, W., Higgins, W., Janowiak, J., Mo, K. C., Ropelewski, C., Wang, J., Leetmaa, A., Reynolds, R., Jenne, P., and Joseph, D.: The NCEP/NCAR 40-year reanalysisproject, B. Am. Meteorol. Soc., 77, 437–471, 1996.
Kerr-Munslow, A. M. and Norton, W. A.: Tropical wave driving of the annual cycle in tropical tropopause temperatures. Part 1: ECMWF analyses, J. Atmos. Sci., 63, 1410–1419, 2006.
Li, F., Austin, J., and Wilson, J.: The strength of the Brewer–Dobson circulation in a changing climate: a coupled chemistry model simulation, J. Climate, 21, 40–57, 2008.
Lin, P., Fu, Q., Solomon, S., and Wallace, J. M.: Temperature trend patterns in Southern Hemisphere high latitudes: novel indicators of stratospheric changes, J. Climate, in press, doi:10.1175/2009JCLI2971.1, 2009.
Mears, C. A., Schabel, M. C., and Wentz, F. J.: A reanalysis of the MSU Channel 2 tropospheric termperatue record, J. Climate, 16, 3650–3664, 2003.
Meehl, G. A., Covey, C., McAveney, B., Latif, M., and Stouffer, R. J.: Overview of the coupled model intercomparison project, B. Am. Meteorol. Soc., 86, 89-93, doi:10.1175/BAMS-86-1-89, 2005.
Ramaswamy, V., Schwarzkopf, M. D., and Randel, W. J.: Fingerprint of ozone depletion in the

spatial and temporal pattern of recent lower-stratospheric cooling, Nature, 382, 616–618, 1996.
Ramaswamy, V., Schwarzkopf, M. D., Randel, W. J., Santer, B. D., Soden, B. J., and Stenchikov, G.: Anthropogenic and natural influences in the evolution of lower stratospheric cooling, Science, 311, 1138–1141, 2006.
Randel, W. J., Wu, F., Nedoluha, G., Vomel, H., and Forster, P.: Decreases in stratospheric water vapor since 2001: Links to changes in the tropical tropopause and the Brewer–Dobson circulation, J. Geophys. Res., 111, D12312, doi:10.1029/2005JD006744, 2006.
Rind, D., Lerner, J., and McLinden, C.: Changes of trace distributions in the doubled CO_2 climate, J. Geophys. Res., 106, 28 061–28 080, 2001.
Rosenlof, K. H. and Reid, G. C.: Trends in the temperature and water vapor content of the tropical lower stratopshere: Sea surface connection, J. Geophys. Res., 113, D06107, doi:10.1029/2007JD009109, 2008.
Salby, M. L. and Callaghan, P. F.: Interannual changes of the stratospheric circulation: Relationship to ozone and tropospheric structure, J. Climate, 15, 3673–3685, 2002.
Shine, K. P., Bourqui, M. S., Forster, P. M. F., et al.: A comparison of model-simulated trends in stratospheric temperatures, Q. J. Roy. Meteor. Soc., 129, 1565–1588, doi:10.1256/qj.02.186, 2003.
Sigmond, M., Scinocca, J. F., and Kushner P. J.: Impact of the stratosphere on tropospheric climate change, Geophys. Res. Lett., 35, L12706, doi:10.1029/2008GL033573, 2008.
Stolarski, R. S., Douglass, A. R., Steenrod, S., and Pawson, S.: Trends in stratospheric ozone: Lessons learned from a 3-D chemical transport model, J. Atmos. Sci., 63, 1028–1041, 2006.
Ueyama, R. and Wallace, J. M.: To what extent does high-latitude planetary wave breaking drive tropical upwelling in the Brewer–Dobson ciculation, J. Atomos. Sci., submitted, 2009.
Yulaeva, E., Holton, J. R., and Wallace, J. M.: On the cause of the annual cycle in tropical lower-stratospheric temperatures, J. Atmos. Sci., 51, 169–174, 1994.

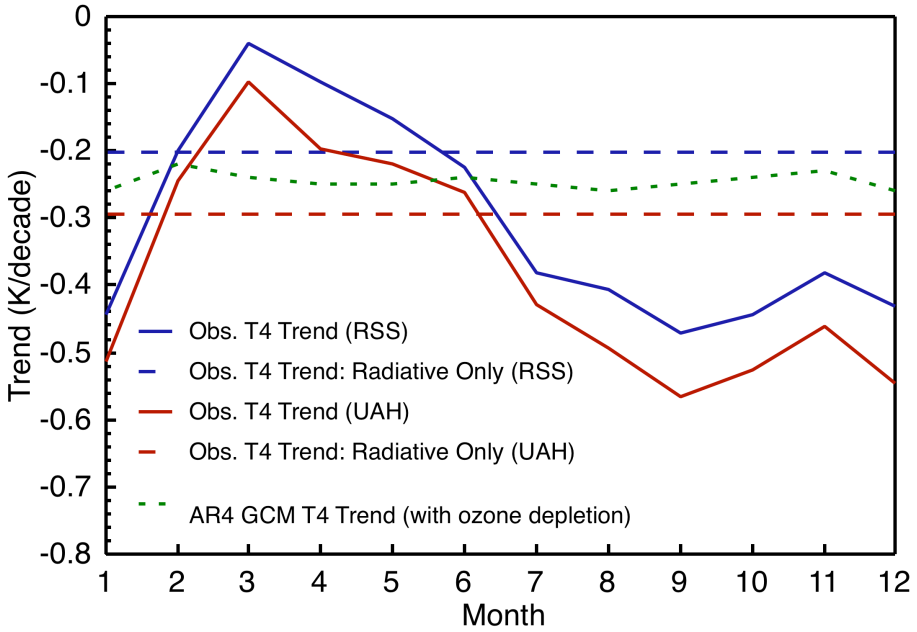

Fig. 1. MSU observed lower-stratospheric temperature (T_4) trends in the tropics (20° N–20° S) for 1979–2007 versus month (solid lines). The dashed lines indicate radiatively induced T_4 trends as derived from this study. The results using RSS and UAH T_4 are presented in blue and red colors, respectively. The green dotted line is the T_4 trend from the IPCC AR4 GCM simulations for a comparison.

ACPD
9, 21819–21846, 2009

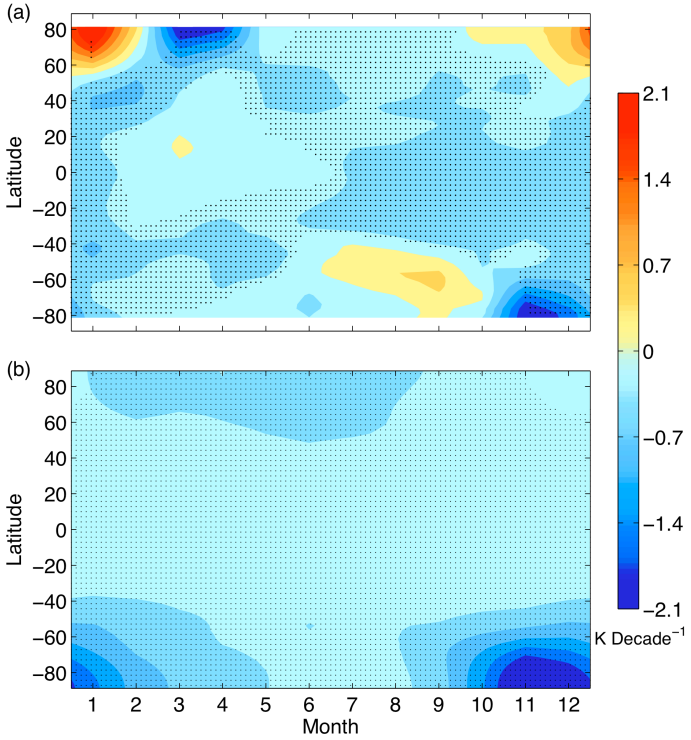

Fig. 2. Zonal mean lower-stratospheric temperature (T_4) trends for 1979–2007 versus month and latitude from **(a)** MSU observations and **(b)** IPCC AR4 GCM simulations that consider ozone depletion. The color contour interval is 0.35 K/decade. The area where trend is significant at 90 and 95% confidence levels by Student's t test is shaded by light and dark dots, respectively. Only RSS MSU T_4 data were used in results presented in Figs. 2–11.

ACPD
9, 21819–21846, 2009

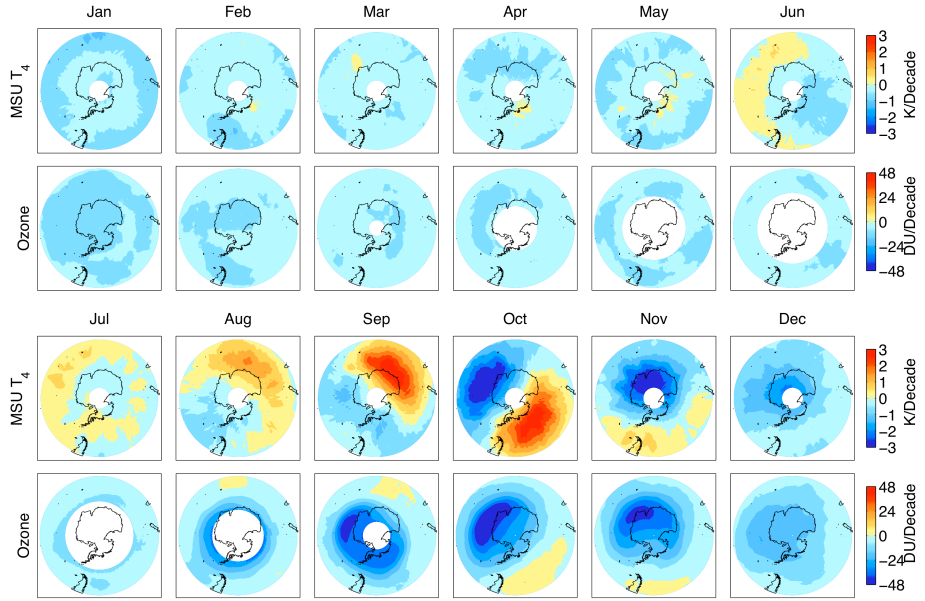

Fig. 3. Monthly trend patterns of MSU lower-stratospheric temperature (T_4) and TOMS total ozone in SH high latitudes for 1979–2007.

ACPD
9, 21819–21846, 2009

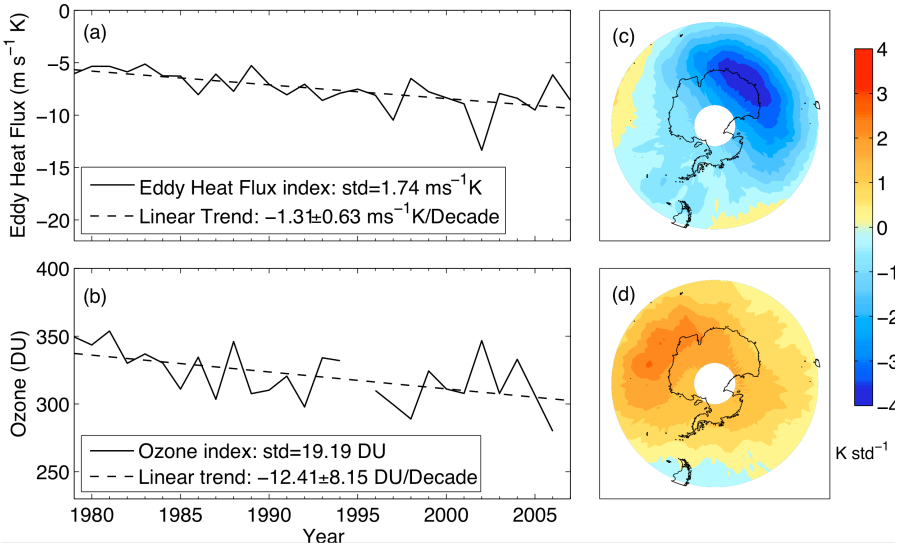

Fig. 4. (a) Time series of the eddy heat flux index and its linear trend in September in southern hemisphere high latitudes. **(b)** Time series of the ozone index and its linear trend in September. **(c)** Map of September T_4 regressed onto the eddy heat flux index in units of K per standard deviation. **(d)** Map of September T_4 regressed onto the ozone index in units of K per standard deviation.

ACPD
9, 21819–21846, 2009

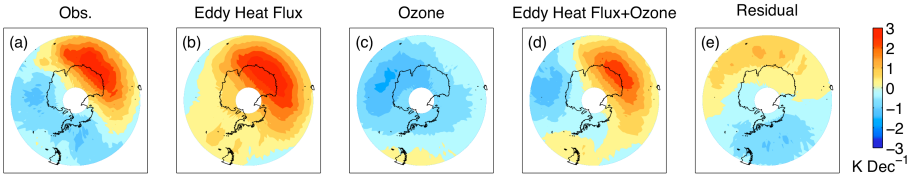

Fig. 5. **(a)** Observed September T_4 trend in southern hemisphere high latitudes. **(b)** T_4 trend attributable to the trend in the BDC as represented by the eddy heat flux index. **(c)** T_4 trend attributable to the trend in ozone. **(d)** linear combination of (b) and (c). **(e)** Residual trend ((a) minus (d)). All trends are in units of K/decade for 1979–2007.

ACPD
9, 21819–21846, 2009

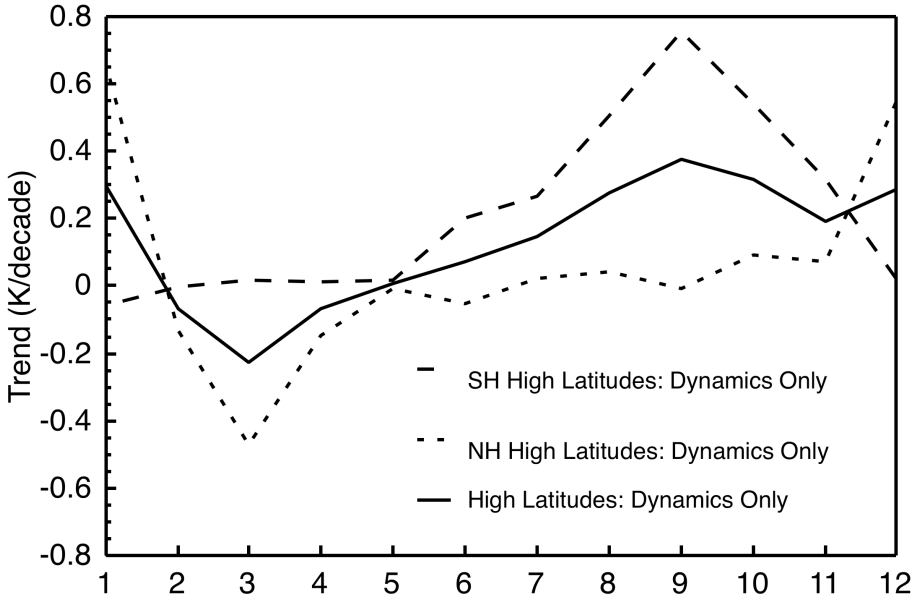

Fig. 6. MSU lower-stratospheric temperature (T_4) trends due to the changes in the BDC in the SH high latitudes (40° S–82.5° S), NH high latitude (40° N–82.5° N), and the high latitudes (40° N–82.5° N and 40° S–82.5° S) for 1979–2007 versus month.

ACPD
9, 21819–21846, 2009

Title Page
Abstract Introduction
Conclusions References
Tables Figures
◄◄ ►►
◄ ►
Back Close
Full Screen / Esc
Printer-friendly Version
Interactive Discussion

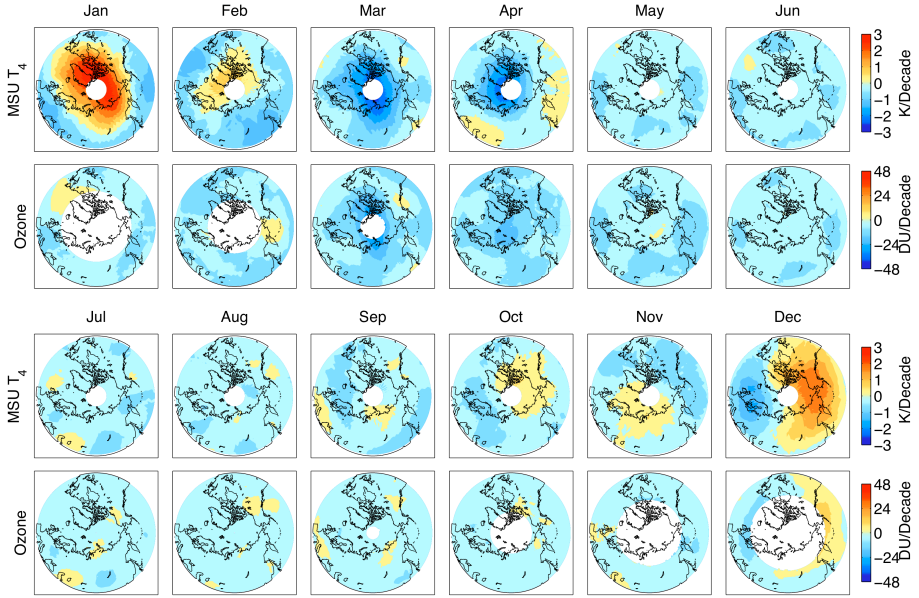

Fig. 7. Same as Fig. 3 except for NH high latitudes.

ACPD
9, 21819–21846, 2009

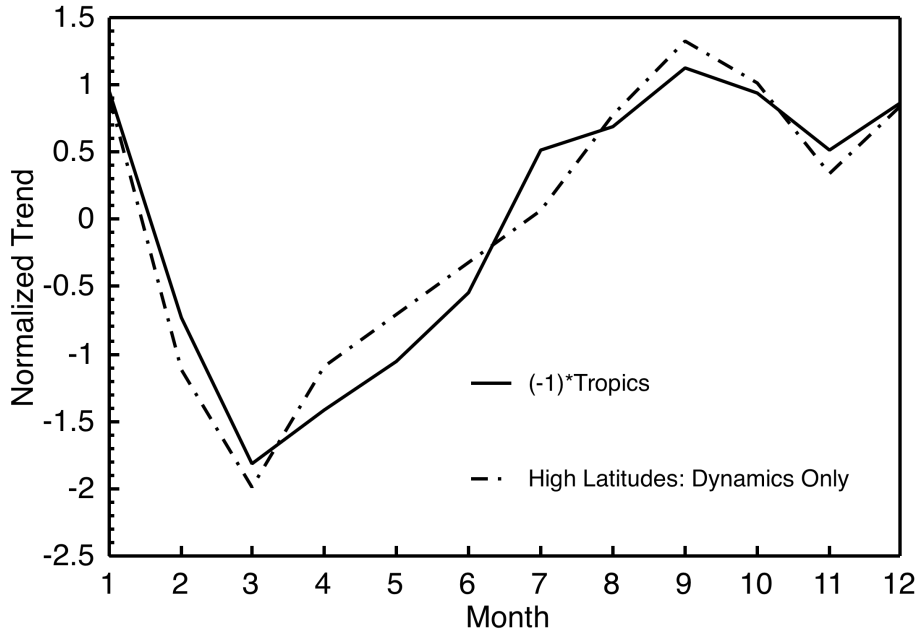

Fig. 8. Comparison of the normalized T_4 trend in tropics multiplied by (−1) and the normalized T_4 trend in high latitudes due to the changes in the BDC for 1979–2007.

ACPD
9, 21819–21846, 2009

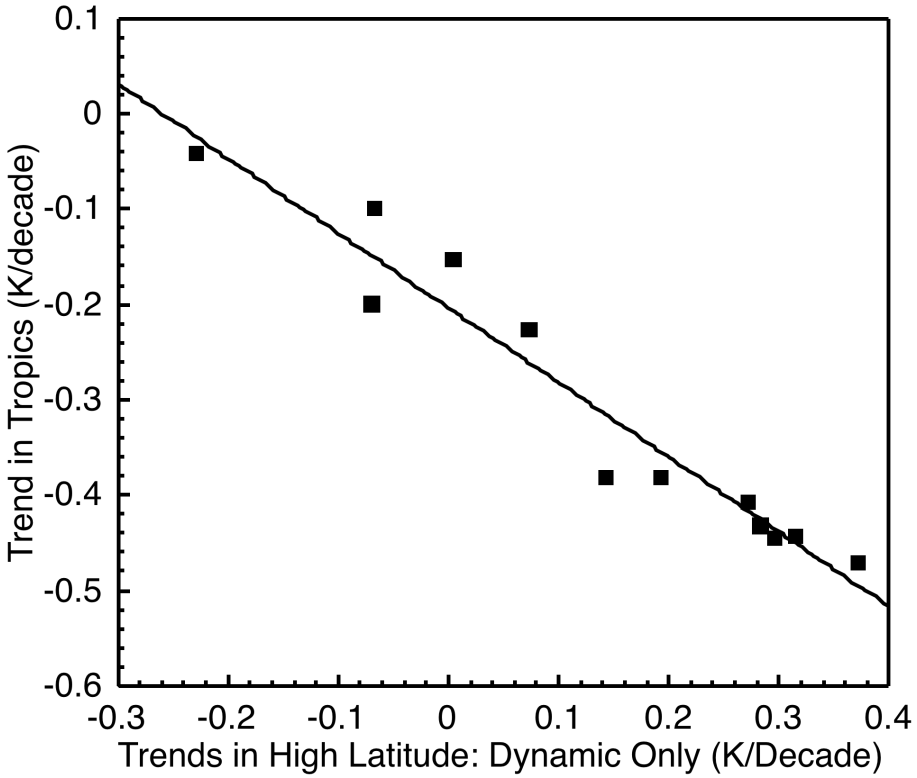

Fig. 9. Trends in tropics (20° N–20° S) versus dynamically induced trends in high latitudes (40° N–82.5° N and 40° S–82.5° S) for 12 months of the year for 1979–2007.

ACPD
9, 21819–21846, 2009

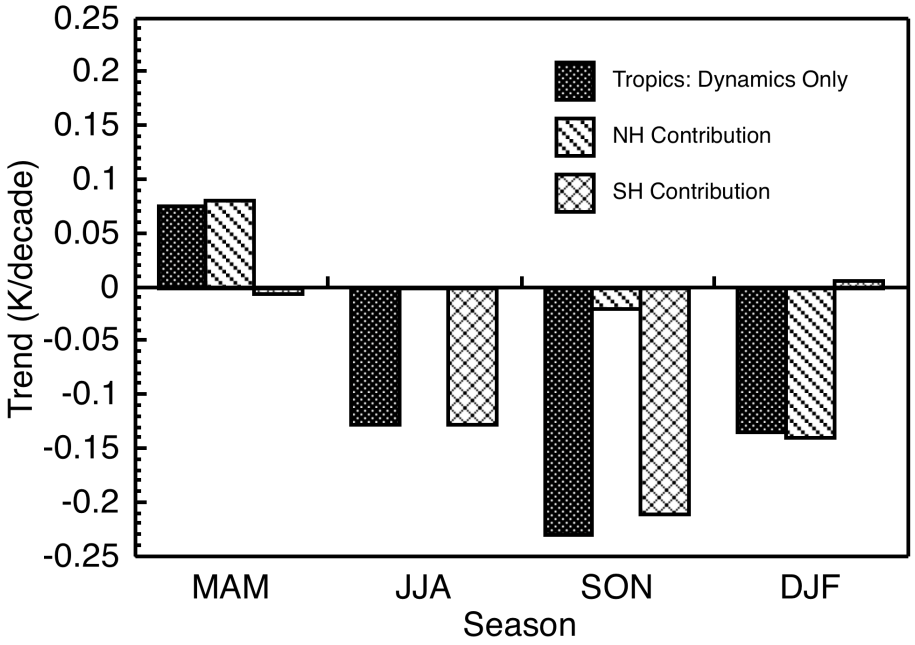

Fig. 10. MSU lower-stratospheric temperature (T_4) trends due to the changes in the BDC in tropics (20° N–20° S) and its contribution from the NH and SH in four seasons for 1979–2007.

ACPD
9, 21819–21846, 2009

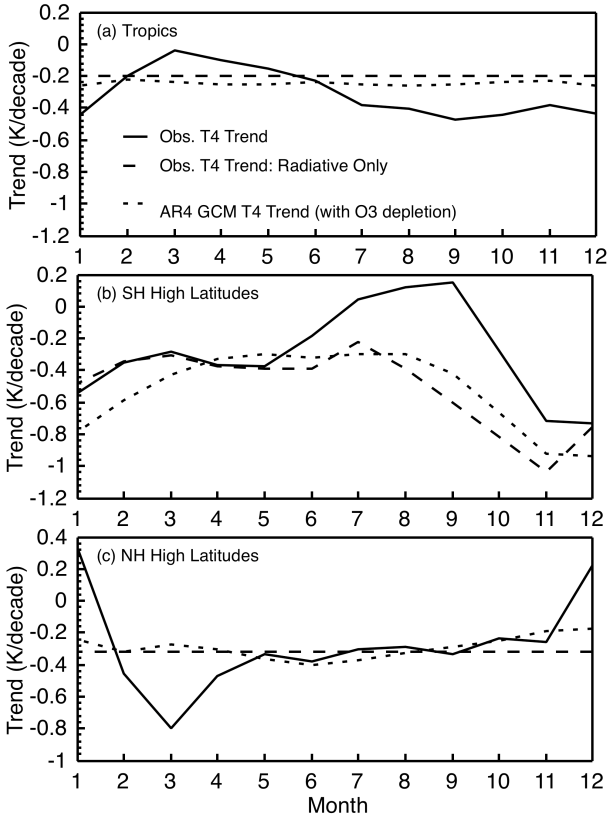

Fig. 11. Compariosn of AR4 GCM simulated T_4 trends with observations for 12 months of the year for 1979–2007 over **(a)** tropics, **(b)** southern hemisphere high latitudes, and **(c)** northern hemisphere hight latitudes. The solid and dotted lines are the T_4 trends from MSU observations and GCM simulations, respectively. The dashed lines are radiatively induced T_4 trends as derived from observations.

ACPD
9, 21819–21846, 2009